Electronic Supplementary Information

A Unipolar Nonvolatile Resistive Switching Behavior in Layered Transition Metal Oxide

Junjun Wang,‡[a,b] Feng Wang,‡[a] Lei Yin,[a,b] Marshet Getaye Sendeku,[a,b] Yu Zhang,[a] Ruiqing Cheng,[a,b] Zhenxing Wang,[a] Ningning Li,[a,b,c] Wenhao Huang,[a,b] and Jun He*[a,b,d]

[a]CAS Center for Excellence in Nanoscience, CAS Key Laboratory of Nanosystem and Hierarchical Fabrication, National Center for Nanoscience and Technology, Beijing 100190, China

[b]Center of Materials Science and Optoelectronics Engineering, University of Chinese Academy of Sciences, Beijing 100049, China

[c]Sino-Danish Center for Education and Research, Beijing 100190, P. R. China

[d]School of Physics and Technology, Wuhan University, Wuhan 430072, P. R. China

†Electronic supplementary information (ESI) available. See DOI: 10.1039/c9nr07456b

‡These authors contributed equally to this work.

*Correspondence and requests for materials should be addressed to J. H. (email: hej@nanoctr.cn).

Supplemental figures

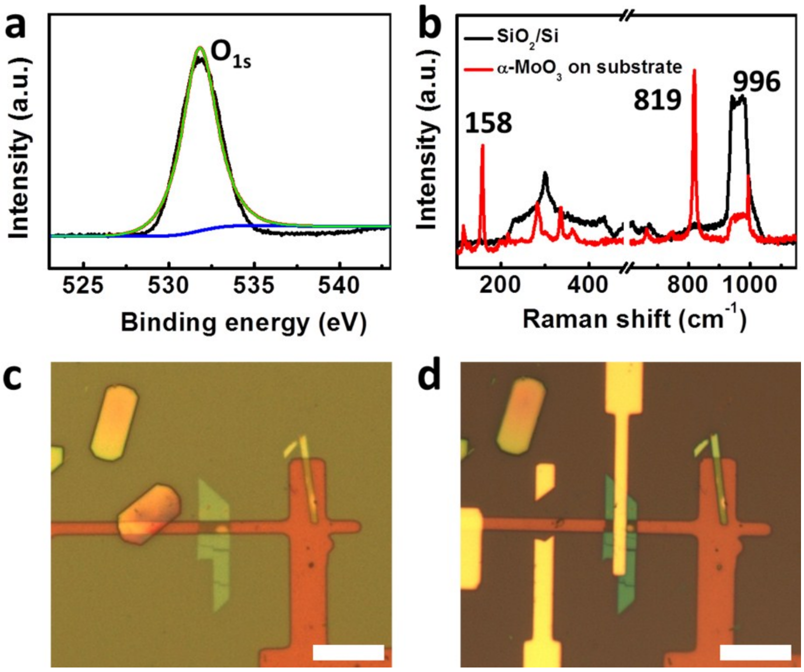

Fig. S1. (a) X-ray photoelectron spectra of O_{1s} XPS peaks with fitted spin-orbit components. Here the α-MoO_3 nanosheet is on mica. (b) The Raman spectra of the α-MoO_3 nanosheet transferred on SiO_2/Si substrate from mica substrate. (c) The optical image of the α-MoO_3 nanosheet transferred on SiO_2/Si substrate from mica substrate and before depositing the top electrode. The scale bar represents 5 μm. (d) The optical image of the α-MoO_3 nanosheet memory cell and after depositing the top electrode. The scale bar represents 5 μm.

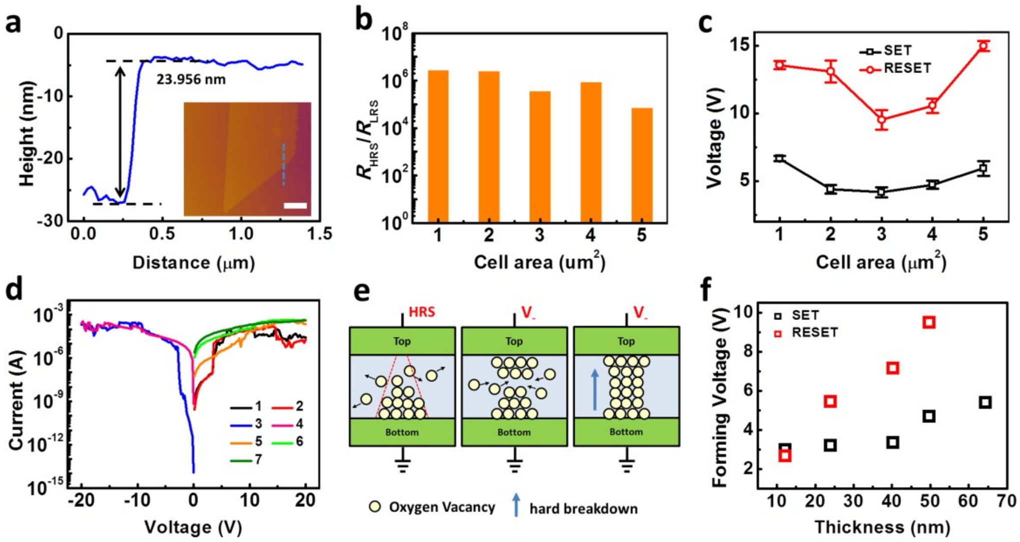

Fig. S2. The electronic characteristics of Au/Cr/α-MoO_3/Au-based memory cells. (a) The thickness profile of the α-MoO_3 nanosheet in Au/Cr/α-MoO_3/Au-based memory cell. The inset shows the corresponding AFM image and a line scan along the dashed blue line. The scale bar is 1 μm. (b)The memory window (R_{HRS}/R_{LRS}) histogram of Au/Cr/α-MoO_3/Au-based memory cells with the cell areas from 1 to 5μm^2. (c) Dependence of the SET and RESET voltage on the cell areas of Au/Cr/α-MoO_3/Au-based memory cells. (d) *I-V* characteristics of another Au/Cr/α-MoO_3/Au-based memory cell. And the number represents the scanning sequence of voltage. (e) The switching mechanisms schematic illustration of device in (d). The top electrode is negative biased and the bottom electrode remains grounded. (f) Dependence of the forming voltage on the thickness of α-MoO_3 memory cells. And the data were extracted from Fig. S3-6.

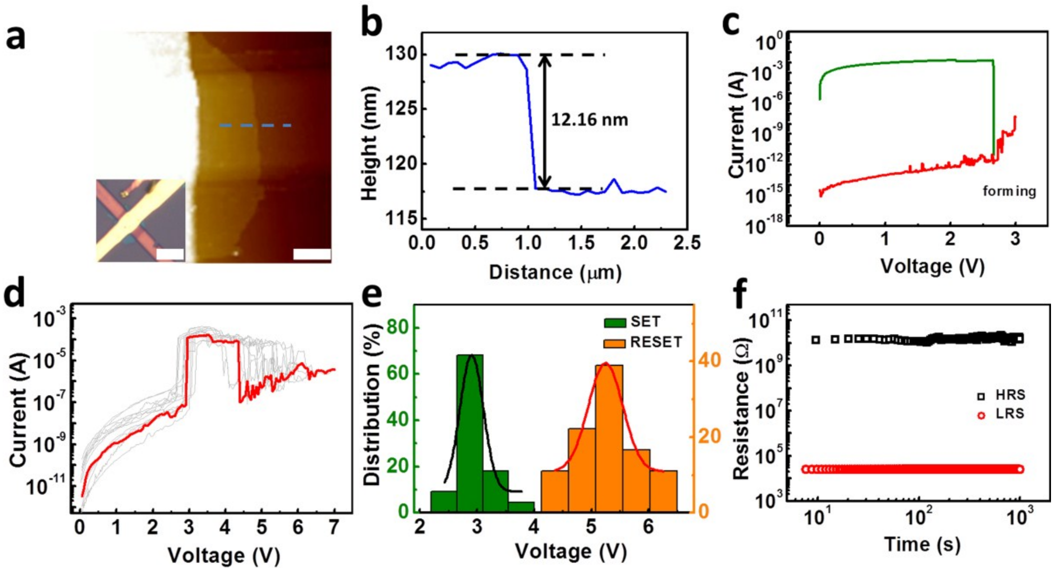

Fig. S3. The electronic characteristics of an Au/Cr/α-MoO_3/Au-based memory cell with 12.16 nm (~6 layers) α-MoO_3. (a) AFM image and a line scan along the dashed blue line. The scale bar is 1 μm. The inset is corresponding optical image of the device and the scale bar is 5 μm. (b) The thickness profile of the α-MoO_3 nanosheet. (c) The electro-forming curve of the device. (d) The *I-V* curves of the device with nonvolatile resistive switching behavior. (e) Distributions of the SET voltage and RESET voltage, which are extracted from (d). (f) Time-dependent measurements of α-MoO_3 crossbar device switch featuring stable retention at room temperature. The resistance of the HRS and LRS is determined by measuring the current at a small bias of 0.01 V.

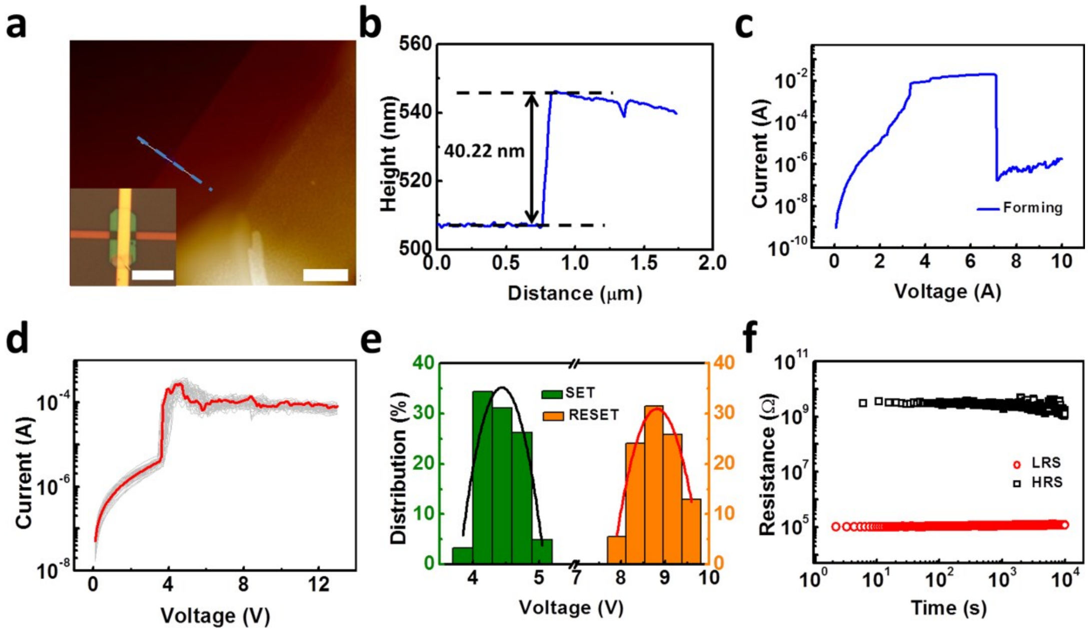

Fig. S4. The electronic characteristics of an Au/Cr/α-MoO_3/Au-based memory cell with 40.22 nm (~29 layers) α-MoO_3. (a) AFM image and a line scan along the dashed blue line. The scale bar is 1 μm. The inset is corresponding optical image of the device and the scale bar is 10 μm. (b) The thickness profile of the α-MoO_3 nanosheet. (c) The electro-forming curve of the device. (d) The *I-V* curves of the device with nonvolatile resistive switching behavior. (e) Distributions of the SET voltage and RESET voltage, which are extracted from (d). (f) Time-dependent measurements of α-MoO_3 crossbar device switch featuring stable retention at room temperature. The resistance of the HRS and LRS is determined by measuring the current at a small bias of 0.01 V.

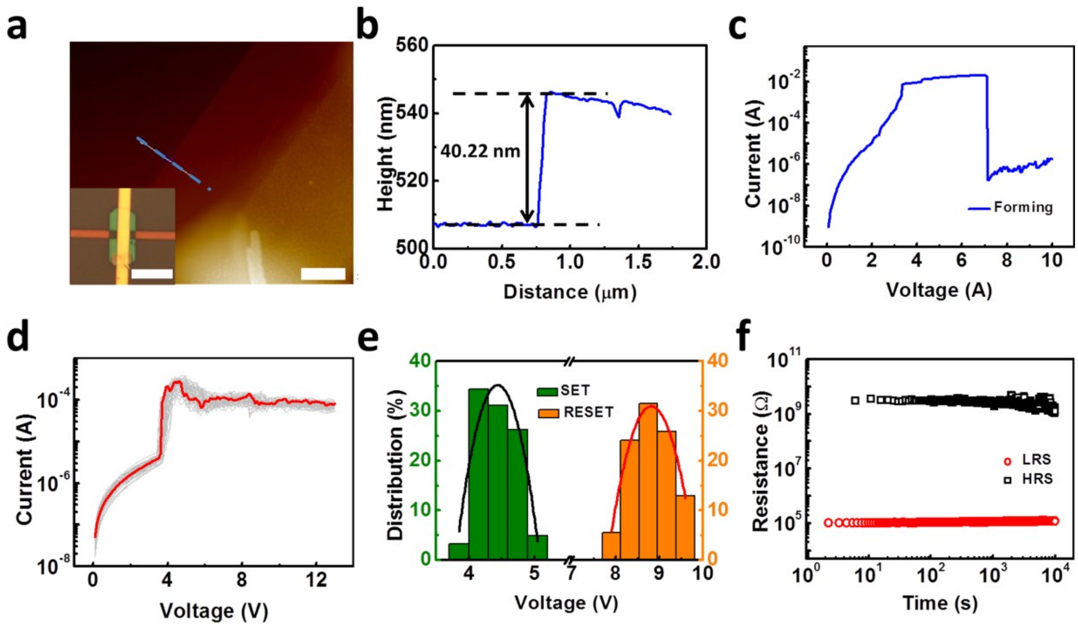

Fig. S5. The electronic characteristics of an Au/Cr/α-MoO_3/Au-based memory cell with 49.74 nm (~36 layers) α-MoO_3. (a) AFM image and a line scan along the dashed blue line. The scale bar is 1 μm. The inset is corresponding optical image of the device and the scale bar is 10 μm. (b) The thickness profile of the α-MoO_3 nanosheet. (c) The electro-forming curve of the device. (d) The *I-V* curves of the device with nonvolatile resistive switching behavior. (e) Distributions of the SET voltage and RESET voltage, which are extracted from (d). (f) Time-dependent measurements of α-MoO_3 crossbar device switch featuring stable retention at room temperature. The resistance of the HRS and LRS is determined by measuring the current at a small bias of 0.01 V.

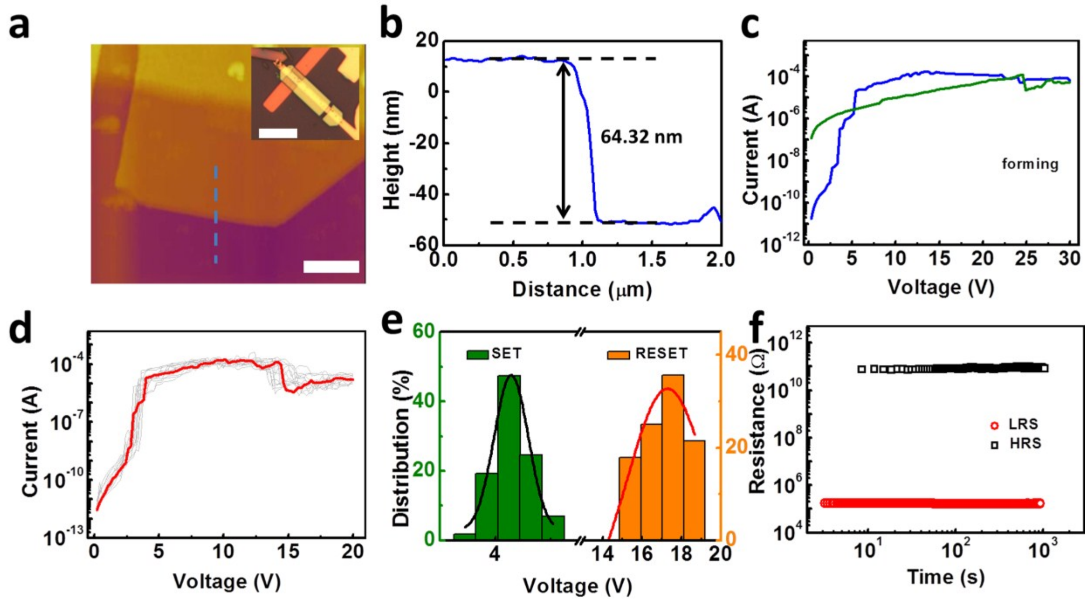

Fig. S6. The electronic characteristics of an Au/Cr/α-MoO_3/Au-based memory cell with 64.32 nm (~46 layers) α-MoO_3. (a) AFM image and a line scan along the dashed blue line. The scale bar is 1 μm. The inset is corresponding optical image of the device and the scale bar is 10 μm. (b) The thickness profile of the α-MoO_3 nanosheet. (c) The electro-forming curve of the device. (d) The *I-V* curves of the device with nonvolatile resistive switching behavior. (e) Distributions of the SET voltage and RESET voltage, which are extracted from (d). (f) Time-dependent measurements of α-MoO_3 crossbar device switch featuring stable retention at room temperature. The resistance of the HRS and LRS is determined by measuring the current at a small bias of 0.01 V.

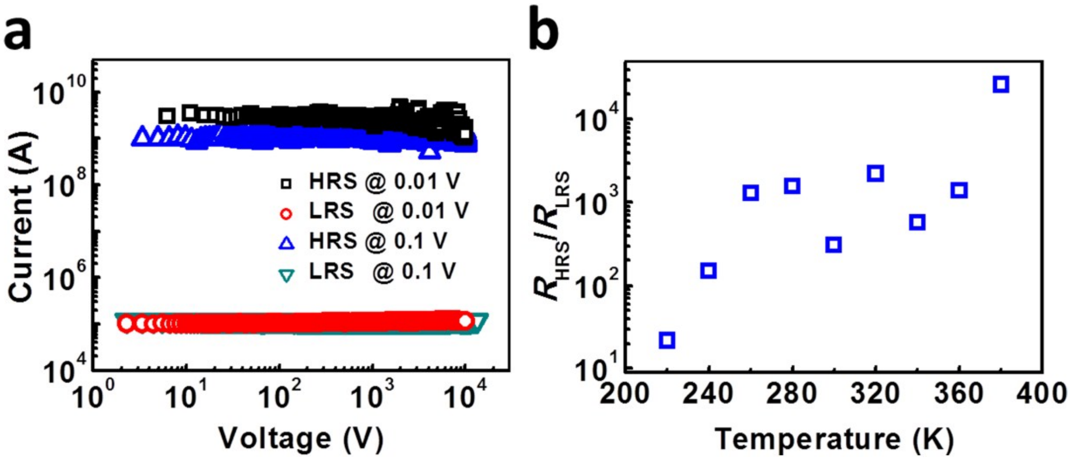

Fig. S7. (a) Time-dependent measurements of α-MoO3 crossbar device switch featuring stable retention at room temperature. The resistance of the HRS and LRS is determined by measuring the current at biases of 0.01 V and 0.1V. (b) Relationship between memory window and temperature.

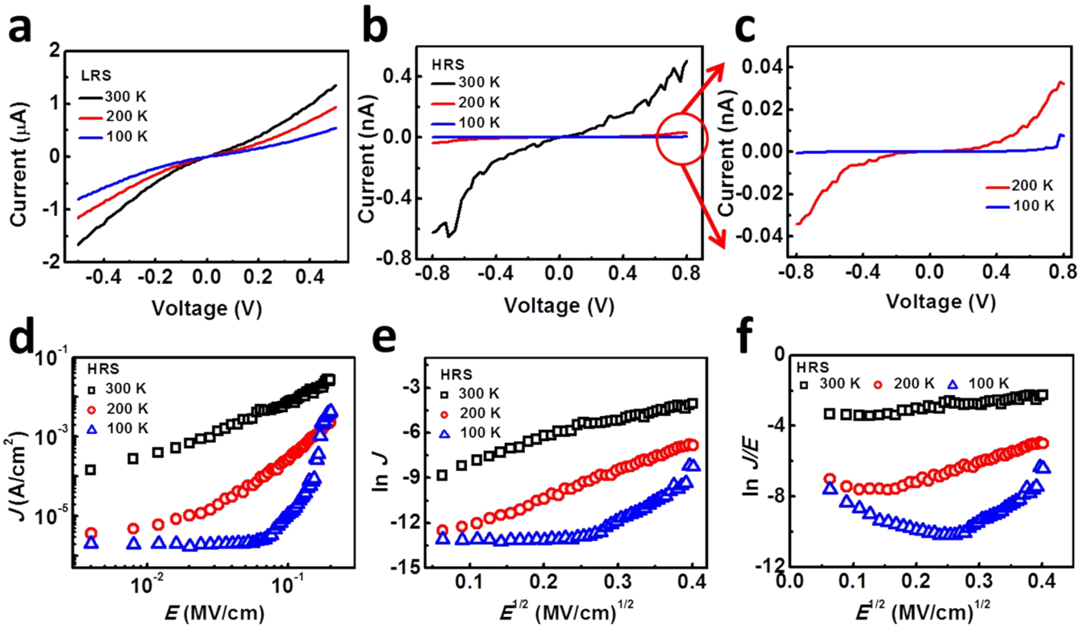

Fig. S8. The conduction mechanism on LRS and HRS of Au/Cr/α-MoO_3/Au-based memory cell. The output characteristic curves of device on LRS (a) and HRS (b-c) at small voltage. In order to analyze the conduction mechanism on HRS, the relationship between current density and vertical electric field is fitted by *J*-*E* (Ohmic conduction (d)), ln$J$-$E^{1/2}$ (Schottky emission (e)), ln(J/E)-$E^{1/2}$ (Poole-Frenkel emission (f)), respectively.

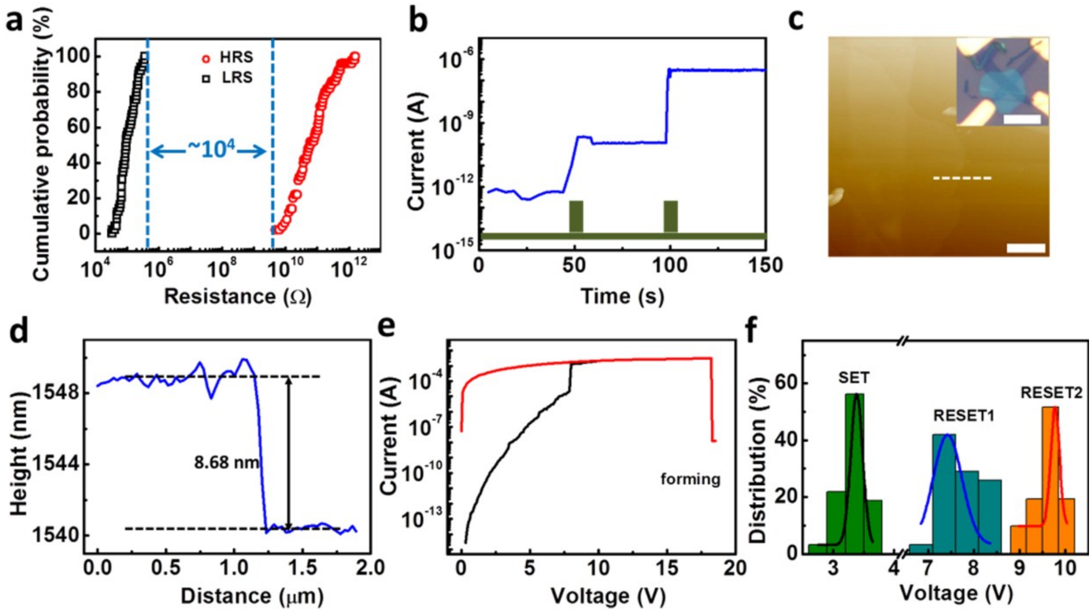

Fig. S9. The multi-bit memory of α-MoO_3 memory cell and the electrical characteristics of devices with graphene electrodes. (a) Resistance distribution of Au/Cr/α-MoO_3/Au RRAM with 50 manual DC switching cycles. (b) The multi-bit memory performance by two continuous voltage pulses with the same duration time (2s) and amplitudes (-6 V). (c) AFM image and a line scan along the dashed white line. The scale bar is 1 μm. The inset is corresponding optical image of a typical graphene/α-MoO_3/graphene crossbar switching device and the scale bar is 5 μm. (d) The thickness profile of α-MoO_3 nanosheet in graphene/α-MoO_3/graphene-based memory cell in (c). (e) The electro-forming curve of the device. (f) Distributions of the SET voltage and RESET1 and RESET2 voltage, which are extracted from Fig. 4c.

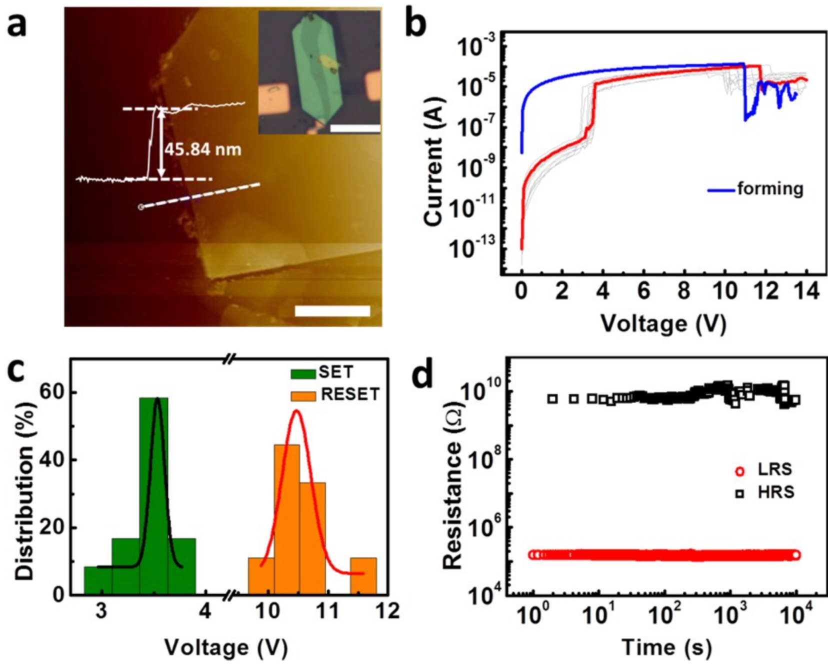

Fig. S10. The electronic characteristics of a graphene/α-MoO_3/graphene-based memory cell with 45.84 nm (~38 layers) α-MoO_3. (a) AFM image and a line scan along the dashed white line. The scale bar is 2 μm. The inset is corresponding optical image and the scale bar is 10 μm. (b) The *I-V* curves of the device with nonvolatile resistive switching behavior. (c) Distributions of the SET voltage and RESET voltage, which are extracted from (b). (d) Time-dependent measurements of α-MoO_3 crossbar device switch featuring stable retention at room temperature. The resistance of the HRS and LRS is determined by measuring the current at a small bias of 0.01 V.

Table S1 The typical memory characteristics based on our device and other amorphous MoOx RRAM

Active material	Active thickness	Device structure	switching mode	Memory window	Time endurance (s)	Reference
CVD α-MoO_3	8.68 nm	vertical	unipolar	$>10^6$	>15 days	This work
CVD MoO_x	~25 nm	vertical	bipolar	$\sim10^3$	10^4	[38]
RF magnetron sputtering MoO_x film	100 nm	vertical	bipolar or unipolar	10~100		[39]
thermal evaporation MoO_x film	~80 nm	vertical	bipolar			[40]
Cu doped MoO_x film	~400 nm	vertical	bipolar	>10	10^5	[41]

Table S1 summarizes the typical memory characteristics of our devices and amorphous MoO_x RRAM from literatures. And the resistive switching mechanisms are as follow:

(i) Our devices: the migration of intrinsic oxygen vacancies;

(ii) CVD MoO_x: the migration of oxygen vacancies produced during the growth process;

(iii) RF magnetron sputtering MoO_x film: the existence of oxygen-deficient sits;

(iv) Thermal evaporation MoO_x film: the excitation of ultraviolet light;

(v) Cu doped MoO_x film: the electrochemical reaction of copper ions.